

RESEARCH PAPER

## Synthesis and Characterization of Schiff-Base Encapsulated Poly Melamine Urea Formaldehyde (PMUF) Self-Healing Nano/Microcapsules

Azhar Abed Salman <sup>1,2\*</sup>, Muhammet Emre Tturun <sup>1,3\*</sup>

<sup>1</sup> Engineering Faculty, Metallurgical and Material Engineering, Karabuk University, 78050, Karabuk, Turkey

<sup>2</sup> Ministry of Oil, Baghdad, Iraq

<sup>3</sup> Eskipazar Vocational School, Karabuk University, 78050, Karabuk, Turkey

### ARTICLE INFO

#### Article History:

Received 29 October 2025

Accepted 06 February 2026

Published 01 April 2026

#### Keywords:

Chitosan

FE-SEM

Nano/microencapsulation

PMUF

XRD

### ABSTRACT

In this work, self-healing materials employ nano/microencapsulation, with a core consisting of Schiff base and a shell made of poly melamine urea formaldehyde (PMUF), synthesized through emulsion polymerization employing redox initiators at low temperatures. These microcapsules were created with various sizes and inhibitor contents, utilizing emulsion polymerization parameters. Schiff-base Synthesized through a series of meticulously controlled steps Chitosan, 1.0 g with 15 mL of deionized water, 1 mL of acetic acid, Cinnamaldehyde, 4.5 mL, and ethanol, 1 mL, was mixed for 30 minutes at 50°C and 600 rpm, yielding a white solution. The addition of (7.5,15 mL of 1.0 M NaOH) to the solution to adjust PH leads to three products code A, B, and C. 100 mL of deionized water and 3.1 gr of surfactant (5.0 gr of Tween 40 + 5.0 gr of Tween 80) for Production of Solution Phase. Then 2.11 cc formaldehyde was mixed with 3.5518 gr of urea, 0.6352 gr of melamine, and 0.2805 gr of ammonium sulfate to Produce of Capsule Phase. 25.08 gr of ammonium chloride and 25.02 gr of resorcinol were mixed with 50 cc of deionized water at 200 rpm. Then, the pH was adjusted to 9.2 using 33% HCl of microcapsules containing Schiff-base. Schiff-base microcapsules were successfully synthesized and characterized, demonstrating stable and uniform properties with effective synthesis confirmed by FTIR, XRD, SEM, FE-SEM, and EDS results. This type of microcapsules improves the performance and durability of coatings.

---

#### How to cite this article

Salman A., Tturun M. *Synthesis and Characterization of Schiff-Base Encapsulated Poly Melamine Urea Formaldehyde (PMUF) Self-Healing Nano/Microcapsules*. J Nanostruct, 2026; 16(2):1526-1537. DOI: [10.22052/JNS.2026.02.004](https://doi.org/10.22052/JNS.2026.02.004)

---

### INTRODUCTION

Self-healing coatings represent a promising advance in coating technology. These coatings incorporate microcapsules filled with healing agents that are activated upon damage. When

the coating is compromised, the microcapsules rupture and release their contents to seal cracks and restore the coating's protective properties. Self-healing coatings could extend the service life of materials by addressing damage proactively and

\* Corresponding Author Email: [memreturan@karabuk.edu.tr](mailto:memreturan@karabuk.edu.tr)

preventing the initiation and spread of corrosion [1-3].

Encapsulated healing agents, such as those in poly (urea-formaldehyde-melamine) microcapsules, release their contents upon capsule rupture, thereby restoring the protective layer. Vascular self-healing systems, where healing agents are distributed through a network of channels, could provide multiple repair cycles by continuously delivering healing agents to damaged areas [4-5].

Thermosetting polymers created through the polymerization of epichlorohydrin and bisphenol-A (BPA). The resulting chemical structure includes reactive epoxide groups, which can cross-link with curing agents such as amines, anhydrides, or polyamides. This cross-linking process is critical in determining the final properties of the epoxy coating.

The type of curing agent used can affect the flexibility, hardness, and chemical resistance of the coating. Amine-based curing agents tend to provide strong chemical resistance, while polyamide-based agents offer better flexibility and toughness.

Fillers and Additives incorporating fillers such as silica, alumina, or carbon fibers and the degree of cross-linking within the coating matrix directly can enhance the mechanical strength, thermal stability, and abrasion resistance of the coating. Additives like plasticizers can improve flexibility, while UV stabilizers can protect against ultraviolet light degradation.

Various researchers have examined multiple healing agents and microencapsulation materials. Necolau et al. [6] demonstrated the application of graphene oxide alongside encapsulated corrosion inhibitors to boost the self-healing process according to their research. As part of self-healing compounds these additives enhance the mechanical behavior while expanding the stability characteristics of the healing platform. Furthermore, in the present investigation additional chemical reaction mechanisms enabled through Schiff-base compounds assist metal ion coordination to improve corrosion inhibition as Abbaspour et al. [7] demonstrated.

Schiff bases exist as a major organic compound family because their imine group (C=N) develops from amine-carbonyl reactions between primary amines and carbonyl compounds including aldehydes or ketones. Schiff bases gained their

name from Hugo Schiff after his initial discovery during the 19th century because these compounds show both versatility and they create strong metal ion complexes. The Schiff base framework consists of  $R_1R_2C=NR_3$  structure which offers multiple substituents  $R_1$ ,  $R_2$ , and  $R_3$  for modifying chemical and physical characteristics of the compound. The chemical properties of Schiff base both in terms of stability and reactivity shift based on whether the aromatic ring contains electron-donating or electron-withdrawing groups. The presence of hydroxyl or methoxy groups attached to the aromatic ring creates more electron density surrounding the imine nitrogen that leads to improved electron interactions with metal surfaces. The imine nitrogen atom becomes more reactive to metal surfaces when electron-donating groups such as hydroxyl ( $-OH$ ) or methoxy ( $-OCH_3$ ) increase electron density in the vicinity. The adsorption behavior of metal surfaces alongside complex formation changes when electron-withdrawing groups like nitro groups reduce electron density. The chelating ability of Schiff bases enables them to create stable coordination complexes with metal ions which stands out as their most prominent characteristic. The ability of Schiff bases to bind with metals creates benefits for corrosion protection because they can develop protective layers on metal surfaces which block corrosion processes. The combination between imine functionality and Schiff base functional groups develops adhesive interactions which stabilize the protective film. The main inhibitive mechanism of Schiff base compounds occurs due to their surface adsorption behavior which establishes protective films above metal surfaces. Participation in adsorption needs chemical interactions between the imine group and either hydroxyl or methoxy functional groups with metal atoms to create coordinated complexes. Metal surfaces receive protection from corrosive elements because this complex creates a barrier which stops water oxygen and chloride ions from entering [8].

Schiff base synthesis occurs through affordable condensation reactions when combining primary amines and carbonyl compounds. The synthesis process takes place at mild temperatures because it facilitates industrial manufacturing. Schiff bases have multipurpose functionality to integrate focused functional groups for specific corrosion protection systems requirements.

Schiff bases exhibit practical uses both in metal surface protective coating additives and in corrosive environments and lubricating fluids and coolants. Protective coatings made with Schiff base additives form bonds with surfaces more efficiently while generating corrosion-blocking layers on material surfaces. The protective films created through Schiff bases application minimize direct contact of corrosion agents with metal surfaces to decrease the corrosion process.

Microcapsules and polymeric frameworks enhance Schiff bases performance when they are incorporated into them. Self-healing protection can now be achieved by physically damaging the coating surfaces because encapsulated Schiff bases become available as polymeric frameworks and microcapsules. This method extends the service time of protective layers. The method produces greatest advantages when mechanical failures frequently occur in locations such as marine and industrial environments [9].

The material Poly(melamine urea formaldehyde)

(PMUF) stands as a widely used product because it possesses distinctive features which enable microcapsule production. Applicable for self-healing coatings because PMUF microcapsules display exceptional durability toward damage and corrosive chemicals across different environmental conditions. The rigid nature of PMUF enables proper entrapping of healing agents and protects them from premature degradation or leakage. Microcapsules produced from PMUF serve as fundamental components for protective coatings which enhance their operational duration.

The microcapsules show outstanding resistance to severe environmental factors which leads them to be employed in vital protection needs against corrosion. The agents packaged within PMUF microcapsules exit these capsules with controlled delivery toward specific areas for maintaining coating preservation [10].

This study aimed to step up the application of Schiff-base microcapsules in self-healing systems by encapsulating PMUF on microcapsules. In



Fig. 1. Washed precipitates from right to left: code A, code B and code C.



Fig. 2. Dried precipitates in the oven, from right to left: code A, code B and code C.

this work, we report a novel chemical interaction mechanism for corrosion inhibition of Schiff based on metals that goes beyond conventional corrosion prevention and self-healing systems. Moreover, due to the controlled release mechanism, these microcapsules release healing agents only when the coating is abraded, thus ensuring the long-term durability of protective layers. The self-healing systems can be much more efficient by means of this approach to the study and have great potential for the development of more sustainable and enduring coatings. It provides an important innovation in the use of microcapsules and corrosion inhibition of Schiff bases from the literature available today.

## MATERIALS AND METHODS

### *Microcapsule Preparation*

The microcapsules were prepared in two stages: Schiff base synthesis and the synthesis of microcapsules filled with Schiff base.

### *Schiff-base Synthesis*

Chitosan, 1.0 g, 15 mL of deionized water, 1 mL of acetic acid, Cinnamaldehyde 4.5 mL, and ethanol, 1 mL, were mixed sequentially over different periods at 50°C and 600 rpm, yielding a white solution after two days of mixing change to dense yellow gel. A 1.0 M NaOH solution 7.5 mL, was added dropwise to the solution and mixed and filtered through filter paper (denoted as Code A), an additional 7.5 mL of 1.0 M NaOH solution, in total 15 mL of 1.0 M NaOH turning its color to white. The second solution was left for 5 hours to allow precipitation to occur. This second solution consisted of two parts of precipitates: one present at the top of the solution (forming at the bottom of the container) denoted as Code B, and the other sediment settled completely at the bottom of the container, denoted as Code C As shown in (Figs. 1 and 2).

### *Production of Solution Phase*

100 mL of deionized water and 3.1 gr of surfactant (5.0 gr of Tween 40 + 5.0 gr of Tween 80) are stirred together for 30 minutes and mixing of Schiff-base(code A, B, C) in solution at a rotational speed of 600 rpm for 22 hours.

### *Production of Capsule Phase*

2.11 cc formaldehyde was mixed with 3.5518 gr of urea, 0.6352 gr of melamine, and 0.2805 gr of

ammonium sulfate at a rotation speed of 200 rpm for 15 minutes. Then, 1.45 cc of 0.1 M NaOH was added to this solution to reach pH 8 and mixed for one hour at a speed of 500 rpm and a temperature of 70 °C. The resulting solution was divided into three parts and dropwise added to three solutions. *Production of microcapsules containing Schiff-base*

25.08 gr of ammonium chloride and 25.02 gr of resorcinol were mixed with 50 cc of deionized water at 200 rpm. Then, the pH was adjusted to 9.2 using 33% HCl. This solution was divided into three parts and added to the three previous solutions in step (b) which had been heated to 55 °C, and mixed for two days at 600 rpm Then, some of the solutions were passed through filter paper, and the remainder was poured into petri dishes and dried at 60 °C for 17 hours.

### *Characterization*

For the examination and characterization of the alloy powder and the microstructure of the coated samples, a Philips-XL30 Scanning electron microscope (SEM) equipped with a Seron - AIS2300C energy dispersive X-ray spectrometer and a Quanta FEG Scanning Electron Microscope (FE-SEM) (model QUANTA FEG-450, FEI Company) coupled with an Energy Dispersive X-ray Spectrometer (EDS) (model Octane Elite, AMETEK Company), was employed. Using the Fourier-transform infrared spectrometer Tensor 27 model by Bruker, Germany, employing a transmission mode in the wavenumber range of 400 to 4000 cm-1 is utilized as a method for determining the structure and measuring chemical species, as well as identifying organic compounds. The phase structure of the powder was analyzed using X-ray diffraction analysis (XRD) with Cu K $\alpha$  radiation (30 mA and 40 kV, Asenware AW-DX300).

## RESULTS AND DISCUSSION

### *Examination of chemical reactions during the production process of microcapsules*

These reactions include the following steps:

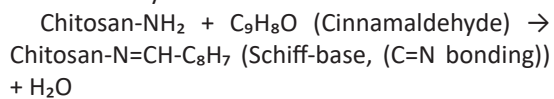
#### *Reaction between Chitosan and Acetic Acid*

$$\text{Chitosan-NH}_2 + \text{CH}_3\text{COOH} \text{ (Acetic Acid)} \rightarrow \text{Chitosan-NH}_3^+ + \text{CH}_3\text{COO}^- \text{ (Chitosan Acetate Solution)}$$

The amine group (-NH<sub>2</sub>) in chitosan reacts with acetic acid to become protonated and turn into chitosan acetate. This process makes the solution suitable for subsequent reactions.

#### Schiff-base Formation Reaction

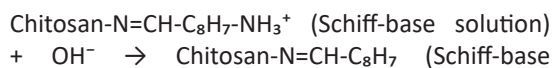
The reaction that occurs after adding to the cinnamaldehyde solution is as follows:



At this stage, cinnamaldehyde ( $\text{C}_9\text{H}_8\text{O}$ ) reacts with the amine group of chitosan to form the Schiff-base (Chitosan-N=CH-C<sub>8</sub>H<sub>7</sub>) compound.

#### Addition of NaOH and Precipitation

After the formation of the Schiff-base, NaOH solution is added dropwise to increase the pH of the solution.



In this step, NaOH solution deprotonates the chitosan Schiff-base, resulting in the formation of insoluble microcapsules. These capsules precipitate out of the solution.

#### Precipitation of Ammonium Salts and Formation of Precipitates

In the final stages of microcapsule synthesis, the following reactions occur:



This stage ensures the complete formation and precipitation of microcapsules. The various precipitates (named Codes A, B and C) correspond to the different stages of microcapsule formation

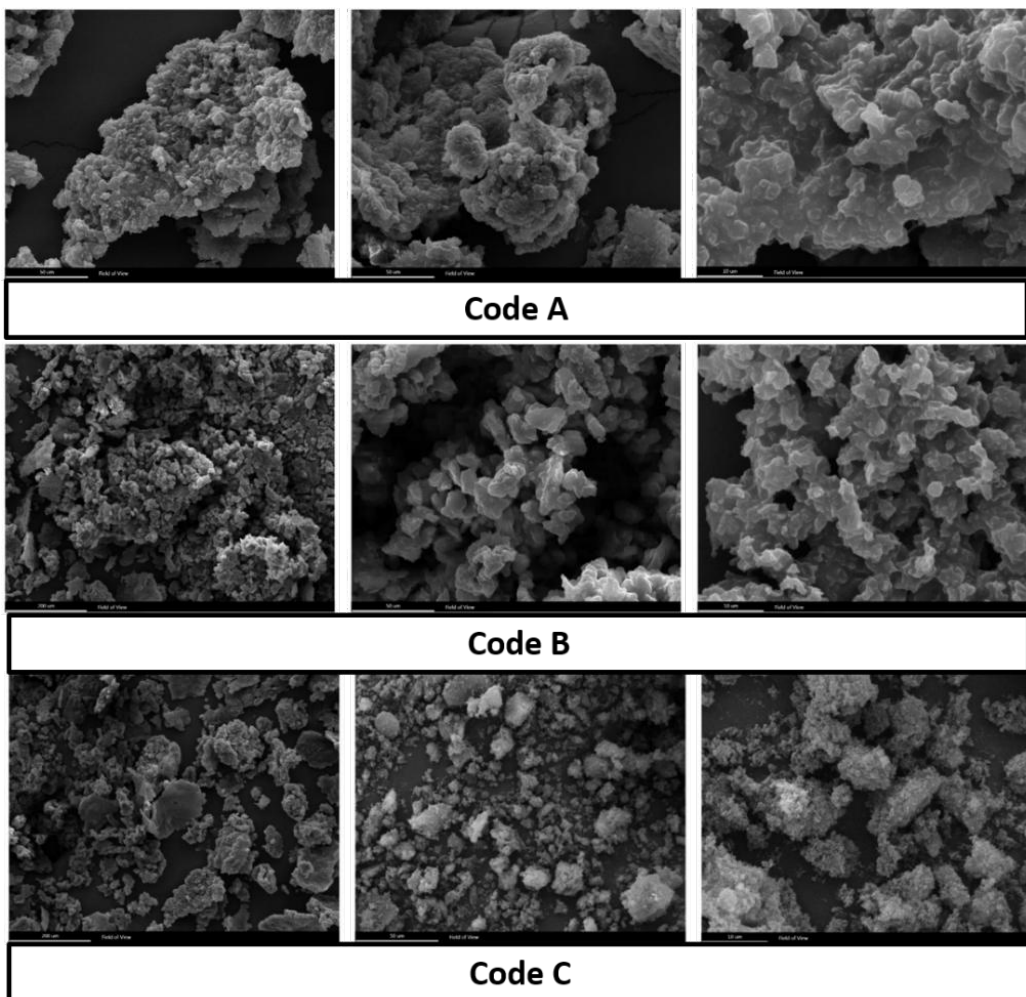


Fig. 3. SEM images of Code A, B and C sample.

and precipitation processes.

#### The surface morphology and structure

SEM images of Code A, B and C sequentially in (Fig. 3). Code A exhibited a relatively smooth surface morphology with minimal aggregation, indicating uniform synthesis conditions. Code B showed a more textured surface, with slight agglomeration observed, possibly due to the complete dissolution during the solution preparation phase. As for the Code C presented a mixed morphology, with both smooth and rough regions, likely due to incomplete dissolution during the mixing phase or varied synthesis conditions.

#### The EDS analysis provided quantitative data on the elemental composition of microcapsules

As shown in Fig. 4, Code A demonstrated consistent elemental distribution with a predominance of carbon (C), oxygen (O), and nitrogen (N), corresponding to the polymeric matrix of microcapsules. Code B also showed a similar elemental composition, with additional peaks corresponding to the Schiff-base compounds, confirming the successful incorporation of these

compounds. Code C displayed a more varied elemental distribution, with some regions showing higher concentrations of certain elements, likely due to the incomplete mixing during synthesis. These results confirm the successful synthesis and elemental incorporation within the microcapsules, though with some variability between the different synthesis conditions. Researchers [11-12] reported analogous EDS spectra in their work on microencapsulation, where the elemental composition confirmed the successful synthesis and encapsulation of organic compounds, reinforcing the validity of these findings.

#### EDS mapping was performed to visualize the spatial distribution of elements

Fig. 5 illustrates the SEM with mapping images of microcapsules for code C. The mapping showed a homogeneous distribution of the key elements (C, O, N), indicating a uniform composition throughout the microcapsules.

#### FE-SEM Morphological Analysis of Microcapsules

FE-SEM images of the morphology of the microcapsules that have been synthesized

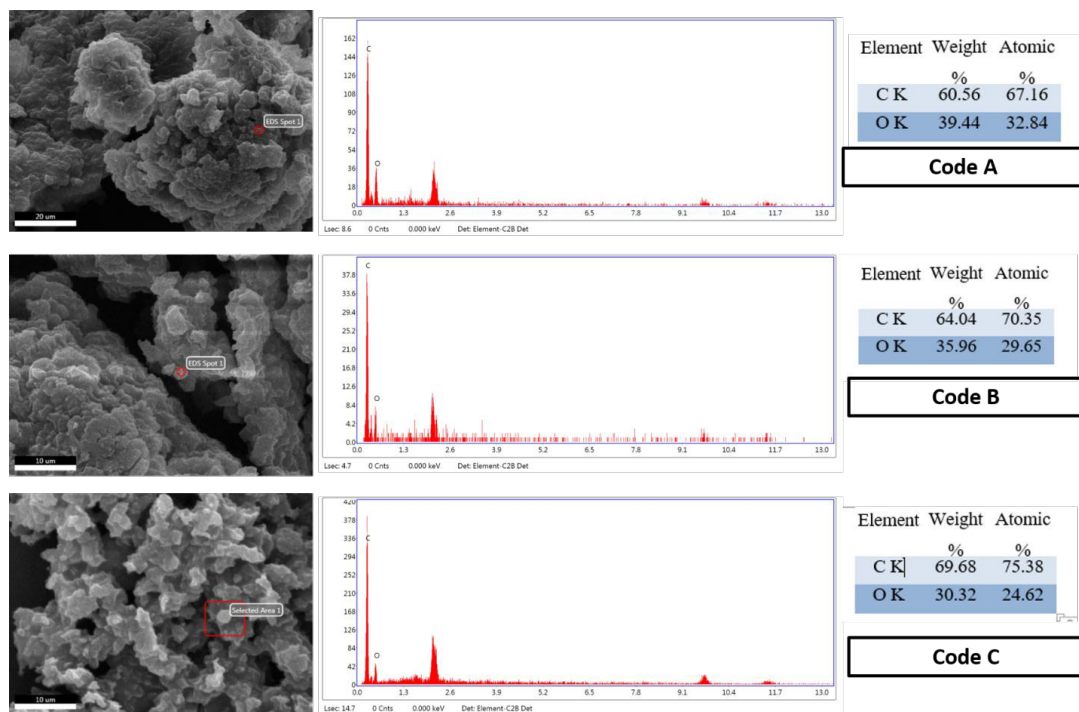


Fig. 4. EDS results from code A, B and C sample.

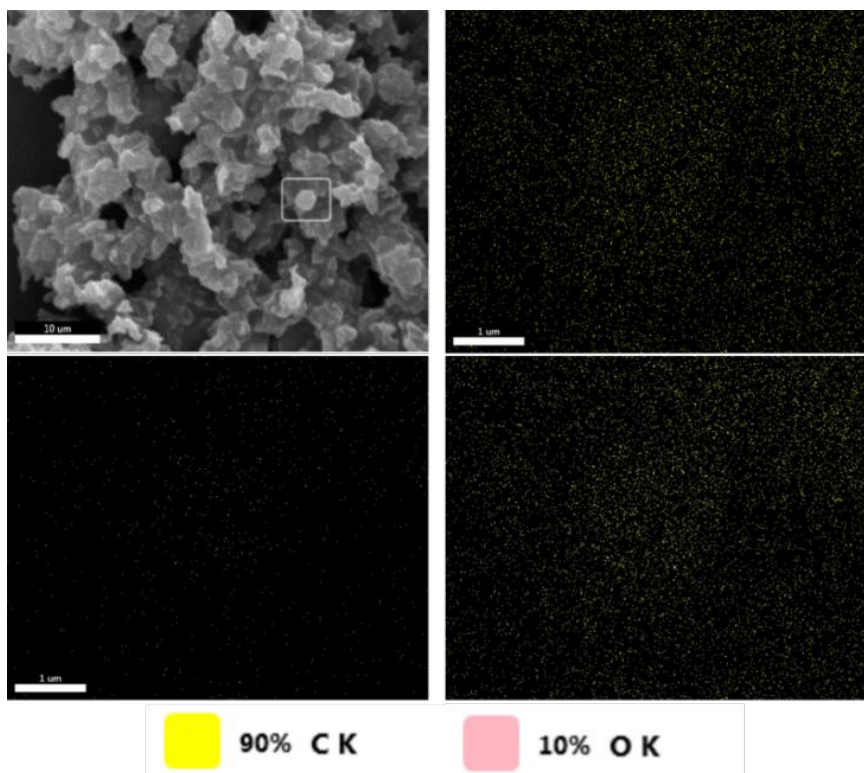


Fig. 5. EDS map results from code C sample.

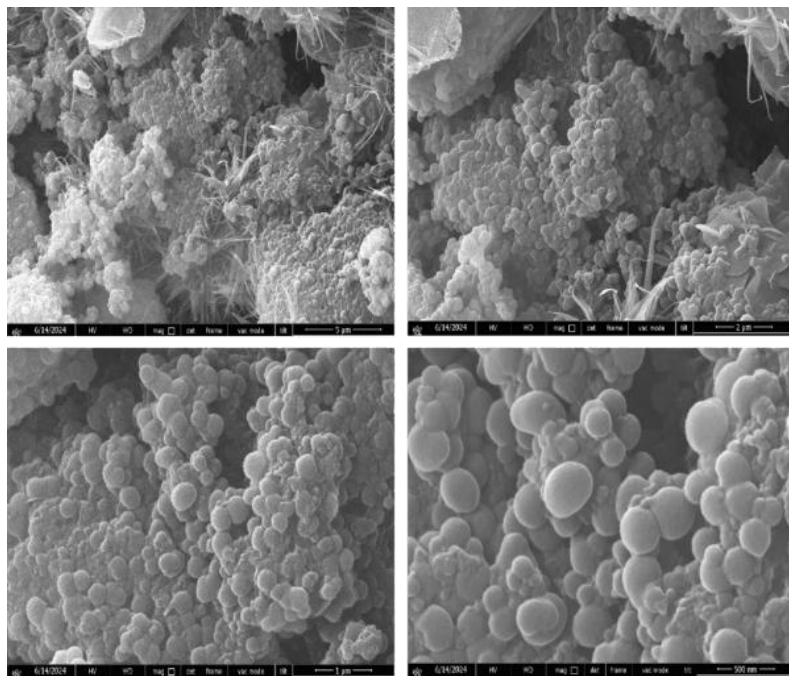


Fig. 6. Precipitates in the Solution.

are observable. At the final stage of synthesis, precipitates from the solution are formed, which are the actual microcapsules that have completely

settled by allowing the solution (suspension) to stand. In Fig. 6, it could be observed that the morphology of the Schiff-base microcapsules is

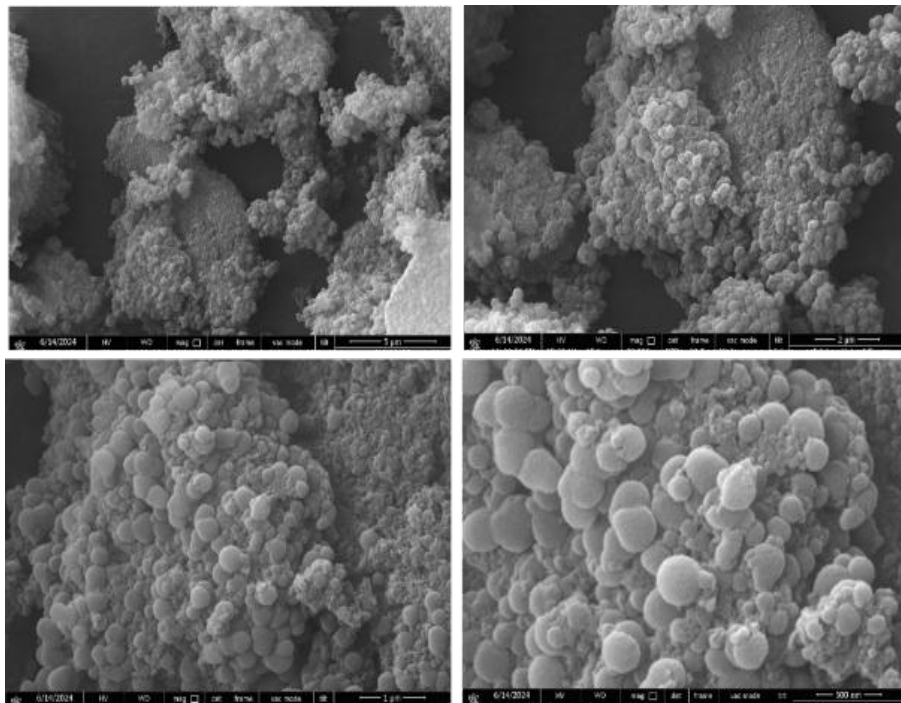


Fig. 7. Synthesized Powder.

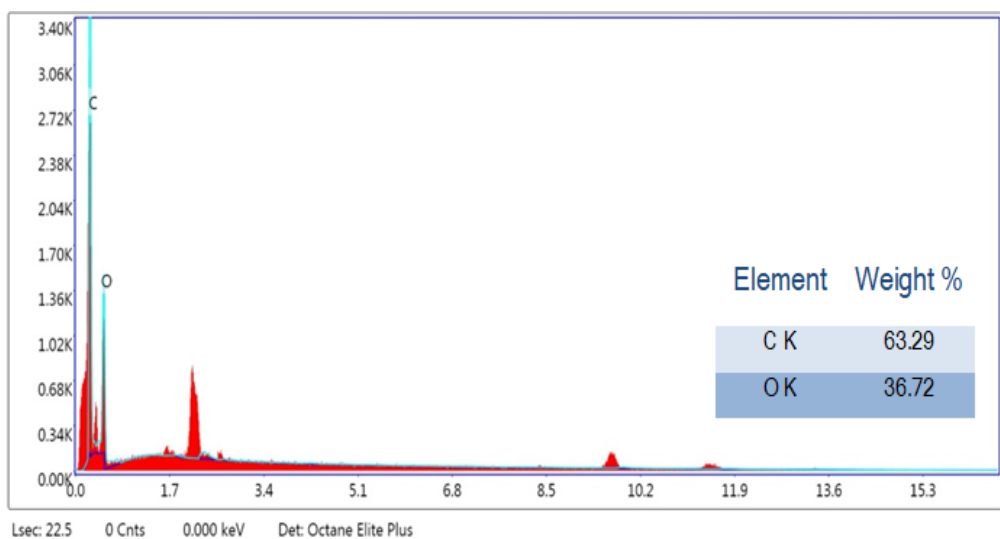


Fig. 8. Elemental Analysis of the Powder Containing Schiff-base Microcapsules.

spherical.

When the microcapsules settled, they were filtered through filter paper and then dried in an oven at 60°C. As shown in Fig. 7, the synthesized powder did not undergo morphological changes due to the heat and remained spherical. Therefore, it could be concluded that this powder will have a desirable performance in terms of morphology because, in microcapsules, the spherical shape could transfer excellent properties to the coating due to its high surface-to-volume ratio and structure compared to other shapes. Based on Fig. 8 and the organic materials used in the synthesis of the powder, it could be concluded that the carbon and oxygen content of 63.29 and 36.72 %wt., respectively, compared to other elements, played a significant role in the formation of microcapsules.

#### ATR-IR Spectrum of Schiff-base Microcapsules

The ATR-IR spectrum of the synthesized

Schiff-base microcapsules powder, depicted in Fig. 9, shows a rich variety of functional groups. This spectrum shows a collection of carbonyl, alkyl, amide, and amine functional groups. The presence of a strong stretching peak at 1037  $\text{cm}^{-1}$  indicates the stretching of C-O-C carbonyl bonds, suggesting the presence of urea and formaldehyde in the microcapsules. The peaks at 1103  $\text{cm}^{-1}$  and 1625  $\text{cm}^{-1}$ , corresponding to C=N and C=N stretching vibrations, highlight the presence of amine and imine groups, which are typical of chitosan and Schiff-base structures. The 1602  $\text{cm}^{-1}$  wave number indicates the stretching bond of amide. These amine and amide bonds indicate the presence of chitosan in the powder containing Schiff base microcapsules [13]. Besides the mentioned functional groups, the alkyl group is also represented as symmetric and asymmetric stretching vibrations at 1448 and 2925  $\text{cm}^{-1}$  wave numbers, respectively. Additionally, the broad peak at 3336  $\text{cm}^{-1}$  is associated with the stretching

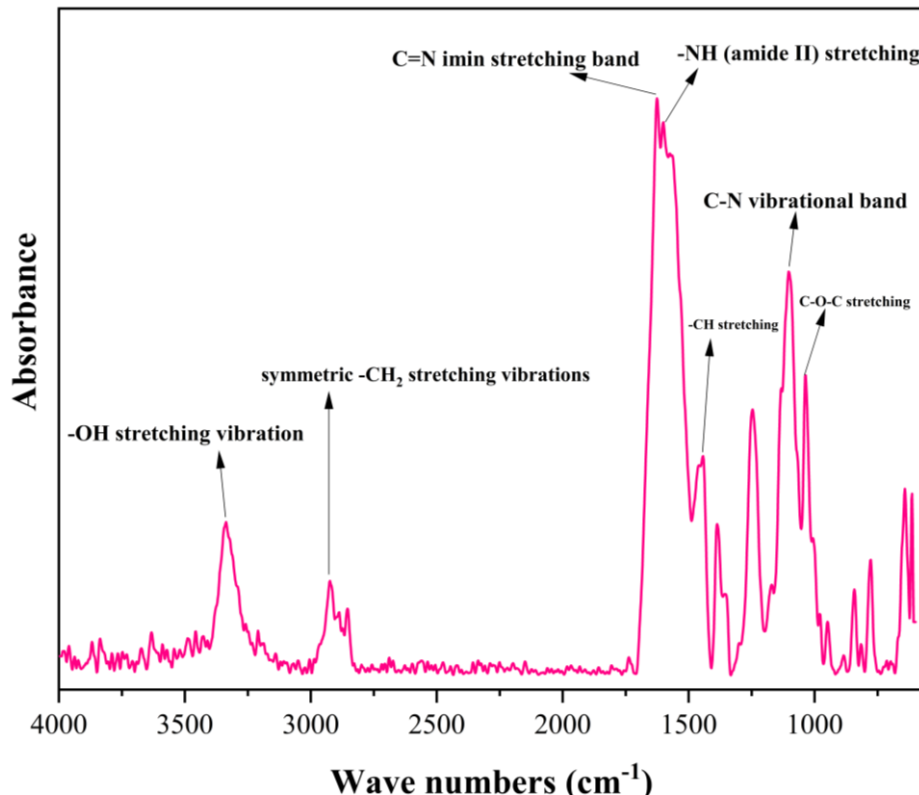


Fig. 9. Attenuated Total Reflectance Infrared Spectrum of the Powder Containing Schiff-base microcapsules.

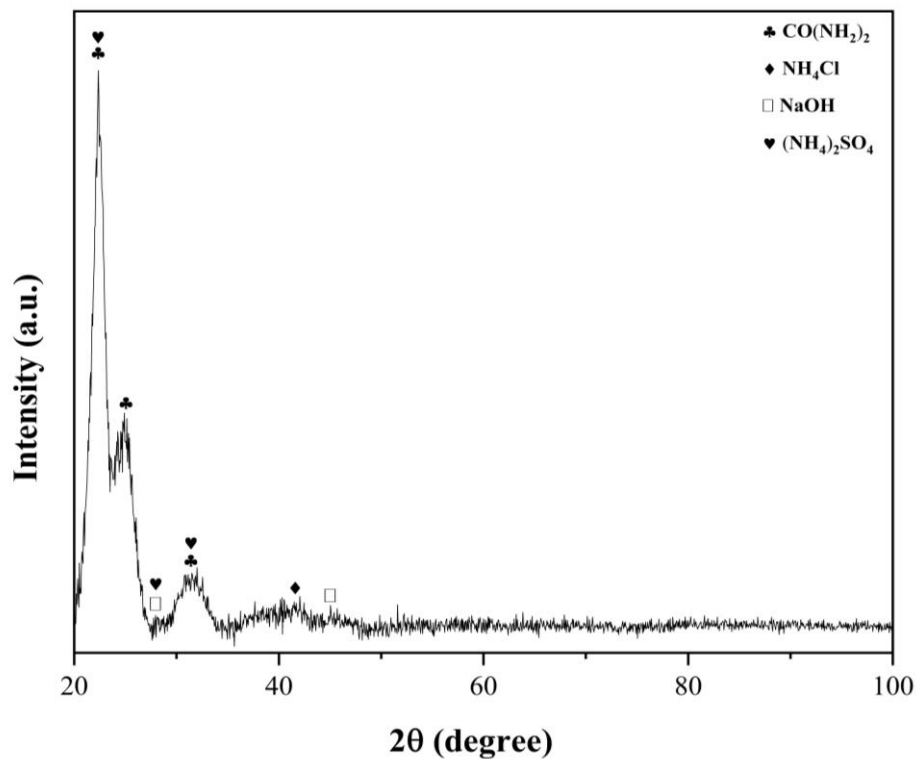


Fig. 10. X-Ray Diffraction Pattern of the microcapsules.

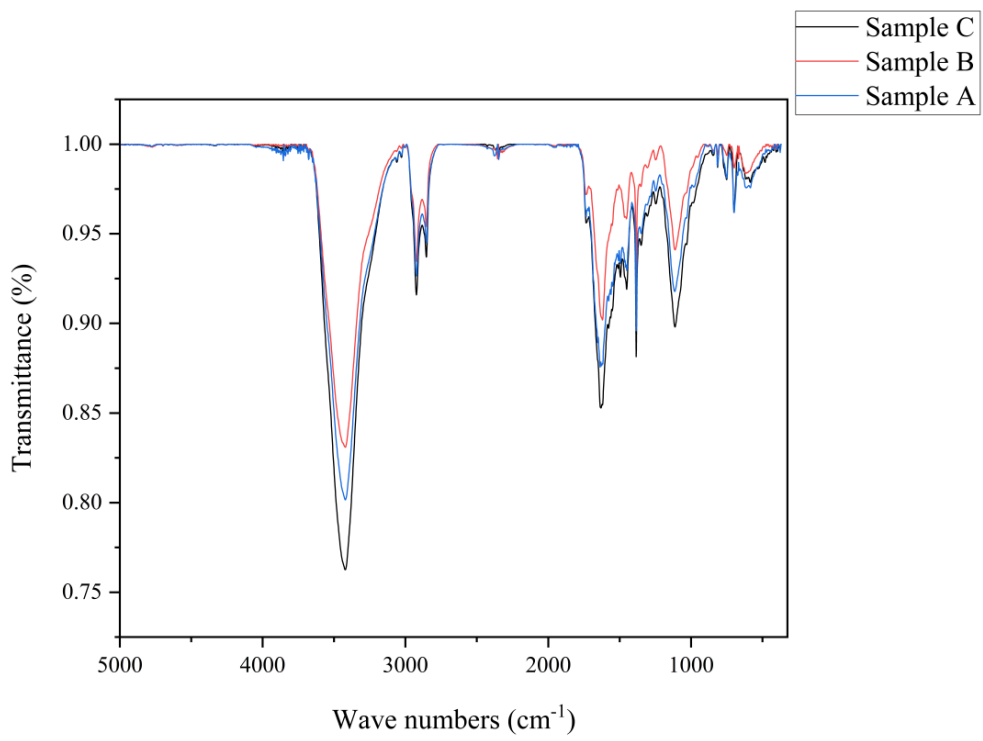


Fig. 11. FTIR Spectrum of Samples Code A to Code C.

O-H bond, indicating the presence of structural water within the microcapsules [14].

#### *The XRD of Microcapsules Analysis*

The XRD pattern of the powder containing Schiff-base microcapsules (Fig. 10) shows significant diffraction peaks at 22°, 25.35°, and 31.15°, which are indicative of the presence of urea, a key reactant in forming the poly(melamine-urea-formaldehyde) shell structure of the microcapsules [15]. Urea's role in the synthesis process is crucial, particularly with the addition of dilute NaOH solution (0.1 M), which facilitates the precipitation of microcapsules by adjusting the pH. However, assigning distinct peaks to NaOH at 28° and 45° is debatable, as NaOH is a highly soluble and amorphous material that does not typically exhibit sharp peaks in XRD. Instead, these peaks may arise from reaction intermediates or side products formed during the microcapsule synthesis [16-17]. The peak at 27.75°, likely corresponds to crystalline by-products such as ammonium chloride or ammonium sulfate, both of which are frequently used in similar synthesis processes and are known to produce distinct diffraction peaks [18]. Ammonium chloride is suggested by the broad hump between 37-42°, while the 27.75° peak is more consistent with ammonium sulfate. These inorganic salts, being highly soluble in water, play a critical role in stabilizing the microcapsules by attracting anions from the solution, thus facilitating better capsule formation and enhancing their structural integrity [19]. These salts aid in microcapsule stability by influencing the solution's ionic environment, improving capsule formation, and enhancing mechanical integrity.

#### *FTIR results of microcapsules*

By comparing the FTIR spectra of samples A, B, and C (Fig. 11), several key differences emerge that could be linked to the synthesis conditions and the resulting material properties. Sample C consistently shows higher intensity peaks across the key regions, including the O-H/N-H stretching, O-H bending, -CH<sub>2</sub> stretching, C=N stretching, and -CH bending regions. This suggests that the synthesis method used for sample C resulted in a material with a higher concentration of functional groups, more pronounced hydrogen bonding, and potentially greater crystallinity [20-21].

## CONCLUSION

1. The synthesis of Schiff-base microcapsules was successfully achieved through a series of meticulously controlled steps, including the preparation of chitosan-based solutions, precise pH adjustments, and thorough mixing and heating processes.

2. NaOH is added to raise the pH of the solution resulting in the formation of distinct precipitates (denoted as Code A, B, and C) correspond to microcapsule formation.

3. SEM analysis in this study reveals a uniform morphology with well-defined microcapsules, indicating a successful encapsulation process.

4. When correlating EDS results with FTIR, the presence of carbon and nitrogen peaks in EDS confirms the organic nature of the microcapsules as identified by FTIR. This combination of data from both techniques ensures that the elemental composition aligns with the expected chemical structure.

5. The morphological analysis of the synthesized Schiff-base microcapsules using FE-SEM revealed that the microcapsules maintained a spherical shape, which is beneficial for coating applications due to their high surface-to-volume ratio.

6. The FT-IR analysis of samples A to C, sample C exhibited higher peak intensities, indicating a more effective synthesis and crystallization behavior. Consequently, the synthesis and sampling method for sample C was selected for further studies due to its superior spectral characteristics.

## ACKNOWLEDGMENTS

This study was carried out as a Ph.D. thesis by Azhar Abd in The Institute of Graduate Programs at Karabuk University, Karabuk, Türkiye.

## CONFLICT OF INTEREST

The authors declare that there is no conflict of interests regarding the publication of this manuscript.

## REFERENCES

1. Functional Coatings: Wiley; 2024.
2. Li J, Shi H, Liu F, Han E-H. Self-healing epoxy coating based on tung oil-containing microcapsules for corrosion protection. *Prog Org Coat.* 2021;156:106236.
3. Nesterova T, Dam-Johansen K, Pedersen LT, Kjil S. Microcapsule-based self-healing anticorrosive coatings:

Capsule size, coating formulation, and exposure testing. *Prog Org Coat.* 2012;75(4):309-318.

4. Shields Y, De Belie N, Jefferson A, Van Tittelboom K. A review of vascular networks for self-healing applications. *Smart Mater Struct.* 2021;30(6):063001.

5. Tan YJ, Wu J, Li H, Tee BCK. Self-Healing Electronic Materials for a Smart and Sustainable Future. *ACS Applied Materials & Interfaces.* 2018;10(18):15331-15345.

6. Necolau M-I, Pandele A-M. Recent Advances in Graphene Oxide-Based Anticorrosive Coatings: An Overview. *Coatings.* 2020;10(12):1149.

7. Abbaspoor S, Ashrafi A, Salehi M. Cathodic disbonding of self-healing composite coatings: effect of ethyl cellulose micro/nanocapsules. *Corrosion Engineering, Science and Technology.* 2021;56(7):659-667.

8. A. Alamiery A. Schiff Bases as Corrosion Inhibitors: A Mini-Review. *Journal of Materials and Engineering.* 2024;2(3):170-185.

9. Umoren SA, Obot IB, Ebenso EE, Obi-Egbedi NO. The Inhibition of aluminium corrosion in hydrochloric acid solution by exudate gum from Raphia hookeri. *Desalination.* 2009;247(1-3):561-572.

10. Ismail NA, Khan A, Fayyad E, Kahraman R, Abdullah AM, Shakoor RA. Self-Healing Performance of Smart Polymeric Coatings Modified with Tung Oil and Linalyl Acetate. *Polymers.* 2021;13(10):1609.

11. Alibakhshi E, Ramezanadeh B, Mahdavian M. Self-Healing Materials in Corrosion Protection. *Self-Healing Smart Materials and Allied Applications*: Wiley; 2021. p. 247-296.

12. Udoji II, Shi H, Daniel EF, Li J, Gu S, Liu F, et al. Active anticorrosion and self-healing coatings: A review with focus on multi-action smart coating strategies. *Journal of Materials Science & Technology.* 2022;116:224-237.

13. Zhang W, Yin L, Zhao M, Tan Z, Li G. Rapid and non-destructive quality verification of epoxy resin product using ATR-FTIR spectroscopy coupled with chemometric methods. *Microchem J.* 2021;168:106397.

14. Ma Y, Zhang W, Wang C, Xu Y, Li S, Chu F. Preparation and Characterization of Melamine Modified Urea-Formaldehyde Foam. *Int Polym Proc.* 2013;28(2):188-198.

15. Dorieh A, Farajollah Pour M, Ghafari Movahed S, Pizzi A, Pouresmaeil Selakjani P, Valizadeh Kiamahalleh M, et al. A review of recent progress in melamine-formaldehyde resin based nanocomposites as coating materials. *Prog Org Coat.* 2022;165:106768.

16. Zhang C, Wang H, Zhou Q. Preparation and characterization of microcapsules based self-healing coatings containing epoxy ester as healing agent. *Prog Org Coat.* 2018;125:403-410.

17. Yan X, Qian X, Chang Y. Preparation and Characterization of Urea Formaldehyde @ Epoxy Resin Microcapsule on Waterborne Wood Coatings. *Coatings.* 2019;9(8):475.

18. Liu T, Liu L. Fabrication and characterization of chitosan nanoemulsions loading thymol or thyme essential oil for the preservation of refrigerated pork. *Int J Biol Macromol.* 2020;162:1509-1515.

19. Kaduk JA, Gindhart AM, Gates-Rector S, Blanton TN. Powder X-ray diffraction of altrenogest,  $C_{21}H_{26}O_2$  Powder Diff. 2022;37(4):240-241.

20. Goyal M, Agarwal SN, Bhatnagar N. A review on self-healing polymers for applications in spacecraft and construction of roads. *J Appl Polym Sci.* 2022;139(37).

21. Stuart BH. *Infrared Spectroscopy: Fundamentals and Applications*: Wiley; 2004 2004/06/25.